Hindawi
Journal of Advanced Transportation
Volume 2021, Article ID 5575537, 14 pages
https://doi.org/10.1155/2021/5575537

Research Article

Dynamic Assessment of Road Network Vulnerability Based on Cell Transmission Model

Yu Sun, Binglei Xie, Shan Wang, and Dazhuang Wu

School of Architecture, Harbin Institute of Technology (Shenzhen), Shenzhen 518055, China

Correspondence should be addressed to Binglei Xie; xiebingleihit@163.com

Received 8 January 2021; Revised 22 March 2021; Accepted 15 May 2021; Published 1 June 2021

Academic Editor: Massimiliano Zanin

The road network maintaining stability is critical for guaranteeing urban traffic function. Therefore, the vulnerable links need to be identified accurately. Previous vulnerability research under static condition compared the operating states of the old equilibrium before the event and the new equilibrium after the event to assess vulnerability ignoring the dynamic variation process. Does road network vulnerability change over time? This paper combines the vulnerability assessment with the traffic flow evolution process, exploring the road network vulnerability evaluation from the perspective of time dimension. More accurate identification and evaluation of vulnerable nodes and links can help to strengthen the ability of road network resisting disturbances. A modified dynamic traffic assignment (DTA) model is established for dynamic path selection (reselect the shortest path at the end of each link) based on the dynamic user optimal (DUO) principle. A modified cell transmission model is established to simulate the traffic flow evolution processes. The cumulative and time-varying index of vulnerability assessment is established from the viewpoint of traveler's time loss. Then the road network vulnerability assessment combined the traffic flow model with the vulnerability index. The road network vulnerability assessment of Bao'an Central District of Shenzhen, China, reveals that road network vulnerability does contain a dynamic process, and vulnerable links in each phase can be exactly identified by the model. Results showed that the road network would have a large vulnerability during the disordered phase when the main road fails. Therefore, prioritizing the smooth flow of main roads can weaken the impact of road network vulnerability exposure.

1. Introduction

Road traffic network is the material basis for the existence and effectiveness of traffic activities. Once the road system suffers from natural disasters, terrorist attacks, traffic accidents, and other disturbances, it can lead to traffic congestion and road disruption, resulting in huge losses to the production and life of residents. Most interference events are uncontrollable. Therefore, it is particularly important to accurately identify the vulnerable links and repair them in a targeted manner. Improving the ability of the road network to resist interference events has attracted increasing attention from scholars in the transportation research field and continuously been applied in the traffic system emergency management field.

Most previous studies evaluated road network vulnerability under static conditions. The key links were identified by comparing the vulnerability assessment indicators of the two equilibrium operating states before and after the event. However, the analysis ignoring the process of evolving from the old to the new equilibrium cannot accurately reflect the changes in traffic service capacity during the sudden event evolution. Will it be more accurate to assess vulnerability from a dynamic perspective?

The goal of the paper can be decomposed into four aspects: First, the dynamic characteristics of road network vulnerability and the factors contributing to vulnerability assessment have been analyzed. Second, the previous static indicators are dynamically adjusted to establish dynamic evaluation indicators for road network vulnerability. Third, a comprehensive road network vulnerability dynamic evaluation model based on the improved traffic flow simulation model combining with the dynamic vulnerability evaluation index is established. Finally, taking the road network in

Bao'an Central Area, Bao'an District, Shenzhen City, as an example to evaluate its vulnerability, the dynamic law of vulnerability changes is summarized, and some suggestions are put forward for decreasing vulnerability.

The structure of the rest paper is as follows. Section 2 reviews existing research of urban road network vulnerability. Section 3 extracts a dynamic evaluation model of road network vulnerability. Section 4 applies the proposed improved model to evaluate the network vulnerability of the surrounding area of Bao'an Center in Bao'an District of Shenzhen City in China and then proposes the analysis of the case results. Section 5 concludes this paper.

2. Literature Review

The two mainstream definitions of vulnerability originate from Berdica [1] and D'Este as well as Taylor [2]. Both types of mainstream definitions take the consequences of road link failure into account, and the difference is whether to consider the probability of failure. Mattsson and Jenelius summarized the current research as a network-based topology and a transportation-based approach [3]. Studies on transport vulnerability have developed over time [4, 5]. The definition of road network vulnerability in this paper is as follows: vulnerability is the nature of a road link with full or partial failure that can significantly reduce the service capacity of the road network or the accessibility of some specific nodes in the road network.

The quantitative analysis of road network vulnerability has gradually developed to the three connotations of vulnerability: firstly, analysis from the perspective of reliability, represented by Bell in this respect, based on pure mathematical graph theory (such as complex network theory) for research [5–13]; secondly, analysis from the aspect of accessibility, represented by Chen, Taylor, and Jenelius, the research based on the cost of road network users and the importance of road sections [2, 3, 14–24]; thirdly, analysis from serviceability, the research based on the road network user cost and road network service level changes [25, 26].

The method of identifying the vulnerable connection through the whole network scanning has two much calculations in the traditional vulnerability analysis; therefore, some scholars have proposed a method for improving the computing efficiency [27, 28]. As there are many types of events that cause road network vulnerability, Jenelius and Mattsson classified the cause of the event and proposed a grid-based method to analyze the combined effects of multiple connections under regional-wide failures [19]. Xiangdong et al. proposed a new redundancy model that can find the best benefit point among travelers and planners effectively, which can also be used to improve and evaluate the vulnerability of urban road network [29].

Cats and Jenelius introduced a dynamic stochastic view into the study of public transport network vulnerability, taking the cumulative effects of interference events on system performance into account [30]. The dynamic evolution of traffic flow and the impact of traffic information on user behavior has gradually been introduced into vulnerability research [31]. Knoop et al. calculated the actual delay of the specific road network after the road link closed by dynamic traffic assignment (DTA) [32]. Cats and Jenelius analyzed the real-time information to promote the transfer of failure effects when the connection fails [30]. Kim and Yeo used a macroscopic basic diagram to observe changes in the traffic image of the road network to identify key links [33].

It can be inferred that using exposure to measure vulnerability under specific conditions has a good effect [16, 34]. Daganzo used the concept of Cell Automata (CA) to discretize the fluid dynamic traffic flow model Lighthill-Whitham-Richards (LWR) and proposed to capture the formation, propagation, and dissipation of queues effectively [35, 36]. Szeto and Wai used the Variational Inequality (VI) to construct the DTA model based on the dynamic user optimal (DUO) criterion and calculate the actual impedance of the path using the cell transmission model (CTM) simulation [37, 38]. Jiang et al. developed a probabilistic approach for assessing transport network vulnerability based on the clonal selection algorithm (CSA) [39].

Most of the existing vulnerability researches are under static conditions, ignoring the evolution process of traffic flow in the disordered phase, and the congestion phenomenon in the evolution process. There is still a lack of research on the dynamic evolution process of traffic flow, and few people have conducted vulnerability assessment from the perspective of the evolution process of traffic flow. Dynamic changes in vulnerability cannot be accurately reflected.

3. Methods

This paper divides dynamically the evolution stage of traffic flow so as to expand the dynamic evaluation results of vulnerability from the time dimension. A new indicator of vulnerability assessment from the perspective of traveler's time loss is established. The DTA model as well as the cellular transmission model is improved to simulate the dynamic evolution process of traffic flow. And the dynamic evaluation model of road network vulnerability is formed.

3.1. Path Selection Model for Vulnerability Assessment. Due to the advantage of Variational Inequality (VI) in dealing with asymmetric problems, it has been widely used in solving DTA problems. Under completely rational assumptions, users will always make the optimal travel choice; that is, the user's travel choice satisfies the DUO condition. According to the first principle of Wardrop equilibrium, the optimal condition of the basic model of DTA can be expressed as

$$f_r^{ij}(k)\left[\eta_r^{ij}(k)-\pi^{ij}(k)\right]=0,$$
$$\sum_{r\in P_{ij}} f_r^{ij}(k)=q^{ij}(k),\ \eta_r^{ij}(k)-\pi^{ij}(k)\geq 0,\ f_r^{ij}(k)\geq 0,\ \pi^{ij}(k)\geq 0,\ \forall r\in P_{ij}, \tag{1}$$

where $\pi^{ij}(k)$ is the shortest travel time of OD pair $i\longrightarrow j$ in time period k, $\eta_r^{ij}(k)$ is the travel time of the feasible path r of OD pair $i\longrightarrow j$ in time period k, $f_r^{ij}(k)$ is the distribution flow of the feasible path r of OD pair $i\longrightarrow j$ in time period k, and $q^{ij}(k)$ is travel demand for OD pair $i\longrightarrow j$ in time period k.

However, the conventional DTA model cannot accurately reflect the changes of various traffic operating parameters in the road network under the influence of the event. Factors such as vehicle retention, queue length limitation, and maximum traffic capacity of the road section need to be considered. Therefore, in view of the impact of the event, this paper makes appropriate adjustments to the DTA model.

3.1.1. Demand Conservation Constraint considering Demand Retention. Affected by the incident, some road links may have travel demand retention. Therefore, the traffic demand in a certain period of time should include not only the traffic flow successfully assigned to the road network but also the retention traffic demand.

$$q_{ij}(k)=\sum_{r\in p_{ij}} f_r^{ij}(k)+q_{ij}'(k), \tag{2}$$

where $q_{ij}'(k)$ is the retention traffic demand for OD pair $i\longrightarrow j$ in time period k.

3.1.2. Association Constraint between Link and Path. The link traffic should equal the sum of all feasible path flows containing this link.

$$x_a(k)=\sum_{i\in I}\sum_{j\in J}\sum_{r\in p_{ij}} f_r^{ij}(k)\delta_{ra}^{ij}(k), \tag{3}$$

where $x_a(k)$ is the flow of road link a in time period k and $\delta_{ra}^{ij}(k)$ determines whether road link a is included in path r.

3.1.3. Road Capacity Constraint and Queue Capacity Constraint. Considering the congestion conditions under the influence of the event, restrictions are imposed on the traffic flow and queuing capabilities of the road link. In the disordered phase, the traffic flow gradually increases but cannot exceed the capacity of the section. With the further increase of vehicles, excessive vehicle density will cause traffic congestion, and the running speed and the actual outflow of the road links decrease, so the vehicle would be queued, but the number of queued vehicles cannot exceed the maximum queue capacity of the road link.

$$x_a(k)\leq C_a(k),$$
$$n_a(k)\leq N_a^{\max}(k), \tag{4}$$

where $C_a(k)$ is the capacity of road link a in time period k, $n_a(k)$ is the actual number of vehicles on road link a in time period k, and $N_a^{\max}(k)$ is the maximum queuing capacity of link a in time period k.

3.1.4. Traffic Demand Time Delivery Constraint. Traffic flow has a dynamic evolution process. In the case of road failure and traffic supply capacity decline, traffic distribution should consider both the traffic demand staying in the previous period and the new traffic demand in the current time. The dynamic traffic allocation method can be used to shift the retained traffic demand to the next time period. This improvement is especially important for the road network vulnerability analysis in the disordered phase. The dynamic assessment of vulnerability needs to meet the constraint shown as

$$q_{ij}(k+1)=q_{ij}^0(k+1)+q_{ij}'(k), \tag{5}$$

where $q_{ij}(k+1)$ is actual traffic demand in time period $k+1$, $q_{ij}^0(k+1)$ is original traffic demand during the time period of $k+1$, and $q_{ij}'(k)$ is unsatisfied traffic demand in time period k.

3.1.5. Traffic Flow Space Propagation Constraint. It takes time for the vehicle to be assigned to the road network to complete the trip in the context of dynamic analysis. During each analysis time period, the vehicle is possible to complete the trip or may only flow into subsequent sections. Therefore, it is necessary to clarify the inflow and outflow relationship between the vehicles and each road link to determine the actual number of vehicles affected in the current period corresponding to the affected degree.

For a certain road link, the number of vehicles in period k should be determined by the number of vehicles in the previous period and the inflow and outflow of the current period.

$$n_a(k+1)=n_a(k)+u_a(k+1)-v_a(k+1), \tag{6}$$

where $u_a(k+1)$ is the inflow of vehicles on link a during the time period $k+1$ and $v_a(k+1)$ is the outflow of vehicles on link a during the time period $k+1$.

The outflow of link a of the path r shall be the same as the sum of the number of vehicles in all subsequent links of the path and the number of vehicles that have completed the trip.

$$v_a^{rij}(k) = \sum_{b \in r'} \left[n_b^{rij}(k) - n_b^{rij}(k-1) \right] + E_r^{ij}(k), \tag{7}$$

where $E_r^{ij}(k)$ is the amount of traffic that completes $i \longrightarrow j$ travel along path r in time period k and r' is the subsequent path of link a in path r.

3.1.6. Other Constraints. The model also needs to satisfy the basic nonnegative constraints and set affiliation and other related constraints.

$$\begin{aligned} & f_r^{ij}(k) \geq 0, \\ & n_a(k) \geq 0, \\ & x_a(k) \geq 0, \\ & u_a(k) \geq 0, \\ & v_a(k) \geq 0, \quad r \in P_{ij},\ i \in I,\ j \in J,\ a \in A. \end{aligned} \tag{8}$$

Travel route selection needs to follow certain traffic distribution rules, as the first-principle requirement of Wardrop equilibrium: all the paths adopted must have the shortest travel time, and the travel time is equal. In this model, it can be expressed as follows: if there is a new vehicle inflow in a road link, the road segment must be included in one of the shortest paths; otherwise, the optimal path selection condition for vehicle inflow will not be added.

$$\begin{aligned} \left[\pi_{hj}^*(k) + \tau_a^*(k) - \pi_{gj}^*(k) \right] u_a^*(k) = 0, \\ u_a^*(k) \geq 0, \\ \pi_{hj}^*(k) + \tau_a^*(k) \geq \pi_{gj}^*(k), \end{aligned} \tag{9}$$

where $\tau_a^*(k)$ is the travel time of link a, $\pi_{hj}^*(k)$ is the shortest travel time of node $h \longrightarrow j$, $\pi_{gj}^*(k)$ is the shortest travel time of node $g \longrightarrow j$, and $u_a^*(k)$ is the vehicle inflow of link a in time period k.

The model needs to be carried out for traffic allocation separately when the vehicle is loaded and at the end of each road link in order to realize the flexible adjustment of the travel path.

3.2. CTM for Vulnerability Assessment. The road network topology has changed during the continuous impact of the road link failure, and travelers go through the process from unknowing to knowing. For the traffic flow in the road network, there were still vehicles flowing into the incident road link in the early stage of the incident, then no vehicles flowed out of the incident road link as time passed, and the upstream link of the incident site became congested or even overflowed. Travelers confirm the fact that the road network has failed, and the directly affected vehicles need to leave the incident road link and reselect the route to travel. Vehicles that have not flowed into the incident road link will directly change the travel path. Thereby, the evacuation of vehicles on the accident road link and the reevolution process of the traffic flow of the road network are formed.

As shown in Figure 1, the cellular transmission model can well simulate the evolution of the traffic flow under the influence of the event. Congestion has gradually formed upstream of the event point since the event occurs and dissipates as the vehicle gradually changes the travel path.

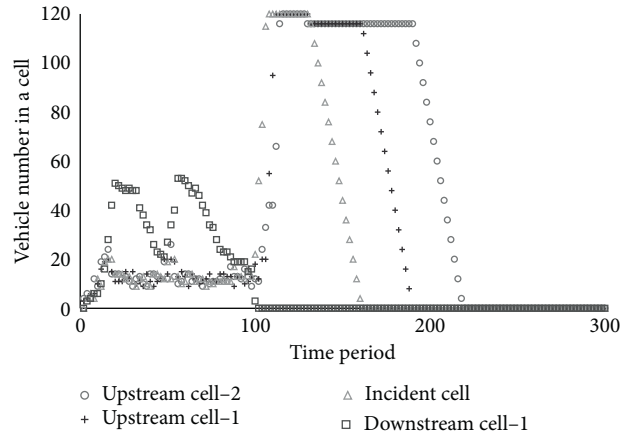

Figure 1: Schematic diagram of the formation and dissipation of congestion on the incident road link.

3.2.1. Cell Transmission Method within the Road Link. When the traffic flow propagates in the road section, CTM expresses the basic propagation relationship of the traffic flow as follows:

$$\begin{aligned} n_i(k+1) &= n_i(k) + y_i(k) - y_{i+1}(k), \\ y_i(k) &= \min\{n_{i-1}(k), Q_i(k), N_i(k) - n_i(k)\}, \end{aligned} \tag{10}$$

where $n_i(k)$ is the number of vehicles in the i-th cell in the time period k, $y_i(k)$ is the outflow of vehicles in the i-th cell in the time period k,$Q_i(k)$ is the capacity of the i-th cell in the time period k, and $N_i(k)$ is the maximum number of vehicles that the i-th cell can hold in the time period k.

Since the LWR model assumes that the traffic flow is a continuous fluid, its solution is relatively complicated. In order to simplify the solution of the model, CTM assumes that the traffic flow satisfies the flow-density relationship shown in Figure 2. Formula (11) gives the calculation method of flow under this relationship.

$$q = \min\left\{ v\rho, q_{\max}, w\left(\rho_j - \rho\right) \right\}, \quad 0 \leq \rho \leq \rho_j, \tag{11}$$

where v is the free speed, w is the speed of backward shock wave propagation, and ρ_j is the blocking density.

At this time, the amount of traffic spread between cells satisfies

$$y_i(k) = \min\left\{ n_{i-1}(k), Q_i(k), \left(\frac{w}{v}\right)\left[N_i(k) - n_i(k) \right] \right\}. \tag{12}$$

In order to further clarify the propagation relationship of the traffic flow, the maximum output capacity S and the maximum receiving capacity R of the cell are, respectively, given by equations (13) and (14):

$$S_i(k) = \min\{ n_i(k), Q_i(k) \}, \tag{13}$$

$$R_i(k) = \min\left\{ Q_i(k), \left(\frac{w}{v}\right)\left[N_i(k) - n_i(k) \right] \right\}, \tag{14}$$

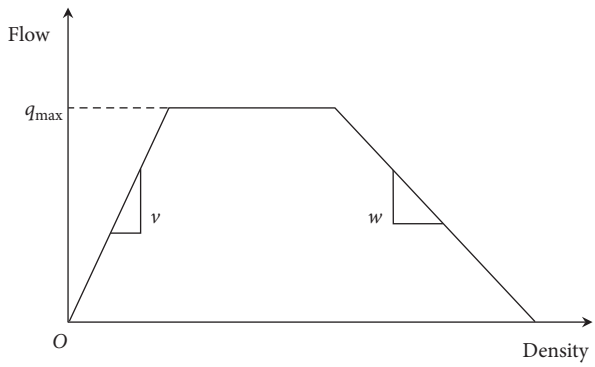

Figure 2: Basic flow-density relationship diagram of CTM.

where $S_i(k)$ is the maximum output capacity of cell i in time period k and $R_i(k)$ is the maximum receiving capacity of cell i in time period k.

The relationship between the flow and the amount of communication between the cells is transformed into

$$y_i(k) = \min\{S_i(k), R_{i+1}(k)\}. \tag{15}$$

3.2.2. Cell Transmission Method between Road Links. The transmission of vehicles between road links includes two forms: merging and diversion. The basic transmission principle is the same as the transmission process in the road link, but the output capacity constraints of the upstream cells and the receiving capacity constraints of the downstream cells must be satisfied at the same time; that is, the traffic flow propagation relationship should satisfy formulas (16) and (17), respectively.

$$\begin{aligned} &y_{i,j}(k) \le S_{i,j}(k), \\ &\sum_i y_{i,j}(k) \le R_j(k), \quad i = 1, 2, 3, \ldots, \end{aligned} \tag{16}$$

$$\sum_j y_{i-1,j}(k) \le S_{i-1}(k),\ y_{i-1,j}(k) \le R_j(k), \quad j = 1, 2, 3, \ldots. \tag{17}$$

The cell capacity at the intersection cannot reach the same capacity as the cell in the road link. At this time, the maximum output capacity of the cell is calculated as

$$S_i^c(k) = \min\{n_i(k), Q_i(k), Q_i^c(k)\}, \tag{18}$$

where $Q_i^c(k)$ is the capacity of the i-th cell at the intersection in the time period k and $S_i^c(k)$ is the maximum output capacity of the i-th cell at the intersection in the time period k.

For the actual road network, formula (19) is always valid, and the cell output capacity can be calculated according to formula (20).

$$Q_i^c(k) \le Q_i(k), \tag{19}$$

$$S_i^c(k) = \min\{n_i(k), Q_i^c(k)\}. \tag{20}$$

The receiving capacity of the intersection cell is calculated according to

$$R_i^c(k) = \left(\frac{w}{v}\right)[N_i(k) - n_i(k)]. \tag{21}$$

Combining the above-mentioned transmission method during link and between links, the basic cell transmission relationship of the traffic flow in the road network is formed.

3.2.3. Vehicle Evacuation Methods on the Accident Road. This paper adds a vehicle evacuation method for interference events based on the basic CTM. For the situation that the road link capacity is greatly reduced, the CTM can naturally capture the increasing amount of vehicle queues in the upstream cell of the road link due to the existence of the road link transmission constraint, and the actual travel time of the road link is gradually extended. The vehicle not arriving at the event-occurred link gradually changed the path according to the DUO condition, and the queue is gradually dissipated because there is no new vehicle flowing into it. In the road link interruption situation, the vehicle upstream of the incident point cannot flow into the downstream cell and stay in the road section. In order to make the simulation results more realistic, it is necessary to add a method to make the vehicle know the link interruption and then turn around and leave the event-occurred link.

(1) The Method of User Knowing the Invalid Link and Reselecting the Path The cell transit ability of the cell is 0 at first. After the time of T, since the incident occurs at time k_a, the road Bottom Vertex (BV) detects that the vehicle outflow is zero, or the road Top Vertex (TV) meets that the number of vehicles in the cell (n) equals the number of vehicles that the cell can accommodate (N). At this time, the vehicle knows that the road link is interrupted, and the new path is selected according to the new road network connectivity.

(2) The Method of the Vehicle Turning around in the Upstream Cell. Transfer the reverse method on the upstream cell vehicle queue of the event-occurred link, and the vehicle queue is sorted in reverse order. The updated cell capacity is the capacity after turning around, and reverse transmission is performed according to formula (22). After reaching the top node of the incident link, the shortest path is selected again based on taking this node as a new starting point, and then the destination transmission is continued according to the normal transmission mode. The upstream cell vehicle U-turn driving method can be specified as

$$n_{i-1}(k+1) = n_{i-1}(k) + y_i(k) - y_{i-1}(k), \tag{22}$$

where $n_i(k)$ is the number of vehicles in i-th cell during k period and $y_i(k)$ is vehicle outflow in i-th cell during k period.

3.2.4. Path Travel Time Calculation Method. The path and link impedance can be calculated based on the actual travel time of the vehicle in this paper. Because the model uses a road link-based approach to traffic distribution (every

vehicle completes a road link), it will reselect the shortest path at the end of the road link and continue to travel according to the new shortest path), and then when calculating the actual travel time of the road link, it no longer distinguishes the origin and destination point of the vehicle in the road link from the driving path but counts the running time of all vehicles directly. The path travel time calculation method can be specified as

$$\tau_a(k) = \frac{\sum_{z \in M^a} \tau_z^a(k) \xi_z^a(k)}{\sum_{z \in M^a} \xi_z^a(k)},$$
$$T_{ij}^r(k) = \sum_{a \in A_{ij}^r} \tau_a(k), \tag{23}$$

where $\xi_z^a(k)$ is whether the z-th traveler has completed the travel on link a, $\tau_z^a(k)$ is the actual travel time of z-th traveler completes of the road link a, and $T_{ij}^r(k)$ is the travel time of the path r.

The actual travel time of all the vehicles traveling on link a is counted in the k period, and the average value is taken as the actual travel time on link a of this period. The actual travel time of each path is calculated according to the travel time of the link, which is used as the basis for the existing vehicle to reselect the path and for the new vehicle to select the path.

3.3. Transmission Efficiency Optimization Method. There are two main problems when applying this model to a large-scale road network: the number of feasible paths and the number vehicles adjusting the path in real time are both large. It is necessary to optimize the computational efficiency of the model for the above two problems.

3.3.1. Search Method Based on Path Set Matrix. A path matrix is established in order to reduce the number of calculations when searching the shortest path, and the total feasible paths between all the node pairs are obtained by traversing the entire road network at one time; then the path to the corresponding position is recorded in the path set. Next, the path search range is limited to the existing feasible path in the set when performing traffic assignment. For the case where the number of times of distribution is extremely large, the amount of calculation can be cut down by reducing the number of searches:

$$\mathbf{R} = \begin{pmatrix} P_{11} & P_{12} & \cdots & P_{1n} \\ P_{21} & P_{22} & \cdots & P_{2n} \\ \vdots & \vdots & \ddots & \vdots \\ P_{n1} & P_{n2} & \cdots & P_{nn} \end{pmatrix}; \tag{24}$$

among them

$$P_{ij} = \begin{cases} \varnothing, & i = j, \\ \left\{ r_{ij} | 0 < l\left(r_{ij}\right) < +\infty \right\}, & i \neq j, \end{cases} \tag{25}$$

where R is the road network path set matrix, P_{ij} is the set of feasible paths from node i to j, r_{ij} is the feasible path from node i to j, and $l(r_{ij})$ is the full travel time of the path r_{ij}.

When searching for the shortest path, directly follow the formula (26) to traverse the path set of the corresponding starting and ending points to obtain the shortest path.

$$r_{ij}^*(k) = \left\{ r | l(r,k) = \min_{r \in P_{ij}} \{ l(r,k) \} \right\}, \tag{26}$$

where $r_{ij}^*(k)$ is the shortest path from node i to j in time period k and $l(r,k)$ is the full travel time of the path r.

3.3.2. Feasible Path Node Number Limit. It is important to set the upper limit of the number of nodes in the path reasonably, which can not only reduce the candidate path set, improving the efficiency of establishing the path set matrix, but also increase the traversal calculation amount of each search for the shortest path in the path set, improving model calculation efficiency comprehensively.

Here, the search method based on the path set matrix is adjusted (the node number limit is introduced) and the path set is changed as

$$P_{ij} = \begin{cases} \varnothing, & i = j, \\ \left\{ r_{ij} | 0 < l\left(r_{ij}\right) < +\infty, 0 < m\left(r_{ij}\right) \leq M_{ij} \right\}, & i \neq j, \end{cases} \tag{27}$$

where P_{ij} is the feasible path sets from nodes i to j, r_{ij} is the feasible path from nodes i to j, $l(r_{ij})$ is the travel time of path r_{ij}, M_{ij} is the upper limit of the path nodes number from node i to j, and $m(r_{ij})$ is the number of nodes included in path r_{ij}.

3.3.3. Node Group Division. It is necessary to group these more concentrated nodes reasonably for the large-scale road network, in order to avoid searching for a more tortuous but not feasible path and then select the paths within the group and between groups to form the final travel path.

3.4. Vulnerability Index Calculation Method. Vulnerability evaluation indicators are mainly concentrated in two categories: one is an indicator that starts from the network topology and ignores the characteristics of traffic flow and is suitable for analyzing networks with relatively certain traffic volumes and small changes in traffic; the other is under noncrowded conditions. The traffic performance index reflects the operating status of the composite transportation system and therefore gradually becomes the mainstream of the road network vulnerability evaluation index.

Most of the indicators considering the elements of traffic flow use the number of individuals affected by the event and the degree of individuals affected by the event as basic factors and then combine them in a certain expression form to establish vulnerability evaluation indicators.

$$V = F(n, c), \tag{28}$$

where V is the vulnerability evaluation index, n is the number of individuals affected by the event, and c is the extent to which the individual is affected by the event.

In vulnerability evaluation, it is a commonly used evaluation method to rank the criticality of road sections by measuring the severity of the consequences caused by the incident. Take the traffic flow, traffic demand, population, and other factors of the evaluated area as the basic number of affected individuals, calculate the degree of individual impact from the generalized travel cost, travel resistance, or accessibility loss, and use the product of the two as the basis data to measure the consequences of vulnerability exposure has been widely adopted by scholars.

Therefore, referring to the vehicle inflow and outflow curve shown in Figure 3, vulnerability evaluation indicators are constructed considering two basic factors in this paper, road traffic flow and traveling time consumption, and then discretize them based on their continuous expression. Taking the product of the instant vehicle number and the instant duration dt of a certain link at time t as the instantaneous travel time consumption of the traveler in the road link at that time, its integral is calculated during the whole research period as the traveler's total travel time consumption on the link a in the study period.where a means the occurrence of event a in the road network. When a is 0, it indicates that no interference event occurs, $u_a(t)$ is the cumulative vehicle inflow of the road network at time t, and $v_a(t)$ is the cumulative vehicle outflow of the road network at time t.

$$B_a = \int_0^t [u_a(t) - v_a(t)]\mathrm{d}t, \tag{29}$$

Then discretize the overall travel time consumption of travelers on link a during the study period based on their continuous expression, and bring in the vulnerability calculation:

$$V_B = \frac{B_a - B_0}{B_0}, \tag{30}$$

where B_a is the travel time consumed of the evaluated area when the interference event a occurs, B_0 is the travel time consumed of the evaluated area when no interference event occurs, and V_B is the cumulative vulnerability index of the evaluated area in the research time.

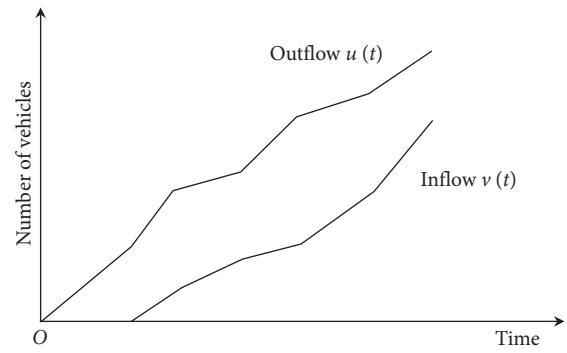

Figure 3: Schematic diagram of the inflow and outflow of vehicles on the road section.

The cumulative travel time of the road network relative to the incremental proportion of the undamaged road network in the study period is used as the cumulative evaluation index of the road network vulnerability, and the ratio of the travel time consumption of the road network under normal and abnormal conditions in the same period is used as the time-varying evaluation index of the road network vulnerability in this paper. The vulnerability assessment index is combined with the traffic flow evolution model to give a calculation method for the vulnerability dynamic indicator value in the model.

Under static conditions, the evaluation indicators of the two equilibrium operating states before and after the event are compared, but the analysis of the static equilibrium conditions implies the assumption that the equilibrium state will be realized, so its conclusion cannot make an accurate evaluation of the road network vulnerability if the equilibrium state has not been realized in the end, and the process of evolving from the old equilibrium to the new equilibrium is ignored. Correspondingly, during the evolution process, the phenomenon that caused traffic congestion was also ignored; therefore, the evaluation results have certain limitations. Therefore, this paper uses dynamic indicators to explore the cumulative and time-varying effects of vulnerability and evaluate the vulnerability of the road network more accurately and comprehensively.

3.4.1. Individual Link Vulnerability Index Calculation Method. The cumulative and time-varying indicators of link vulnerability are shown, respectively, as

$$B_a(k) = T_k[u_a(k) - v_a(k)] = T_k \sum_{i \in I_a} n_i^a(k), V_a = \frac{\sum_k [B_a(k) - B_a^0(k)]}{\sum_k B_a^0(k)}, V_a(k) = \frac{B_a(k) - B_a^0(k)}{B_a^0(k)}, \tag{31}$$

where T_k is the duration of the k-th time period, $n_i^a(k)$ is the number of vehicles in the i-th cell in link a during k period actual, $B_a(k)$ is the total time consumption of the road link a in the k period, where 0 corresponds to the value when no event is affected, V_a is the cumulative vulnerability index value of link a as of k period, and $V_a(k)$ is the time-

varying vulnerability index value of road link a during k period.

3.4.2. Road Network Vulnerability Index Calculation Method. According to the road network structure and the calculation method of the vulnerability index of the road link, the cumulative index and the time-varying index of the road network vulnerability are shown as

$$V_{\text{net}} = \frac{\sum_{a\in A}\sum_{k}\left[B_a(k) - B_a^0(k)\right]}{\sum_{a\in A}\sum_{k}B_a^0(k)},$$
$$V_{\text{net}}(k) = \frac{\sum_{a\in A}\left[B_a(k) - B_a^0(k)\right]}{\sum_{a\in A}B_a^0(k)}, \tag{32}$$

where A is a set consisting of all links in the road network, V_{net} is the cumulative vulnerability index value of road network as of k period, and $V_{\text{net}}(k)$ is the time-varying vulnerability index value of road network during k period.

4. Case Study

4.1. Regional Overview and Parameter Design. The surrounding area of Bao'an Center in Bao'an District of Shenzhen City is selected as an example study object. The boundary of the area is mainly composed of Guangshen Highway, Xixiang Avenue, Haibin Avenue, and Hubin Road, with Bao'an Avenue passing through and the dense branch network matching inside. The area is about 16 square kilometers and the planned permanent population is 380,000. The internal land use types are mainly commercial land near the Qianhai Bay (Binhai area), a large number of residential lands scattered within the area (Bihai area), and parts of school land.

The traffic flow of the study area is mainly composed of a large number of transit traffic flows and some internal traffic trips on Guangshen Highway and Bao'an Avenue. According to the detailed level of OD data, the road network in the area is collated and simplified appropriately based on the actual layout of the road network in Bao'an Central Area, and then the abstraction is the road network structure shown in Figure 4.

The time range is 6:30–9:30 pm, and a blocking density is 133 pcu/ln•km. The remaining parameters are shown in Table 1. Some roads do not have the same section throughout the entire road. The same value is used here to simplify the road network. In addition, for the road links where the road capacity and the free flow speed can be queried, the value is taken according to the actual situation; for the link where the relevant parameters cannot be queried, the value is taken according to the "City Planning Design Code CJJ37-2012." Main interference situation setting is shown in Table 1.

The details of the change process cannot be reflected when the time interval is too large, and it is difficult for the model to achieve the required accuracy if it is too small. This paper has conducted multiple tests based on the road length and speed limit of the studied area based on previous article [37]. According to the principle of speed limit × time interval = cell length, for example, two nodes are separated by 1000 m and are divided into 5 cells with a length of 200 m. The driving distance can be exactly the length of 1 cell in each cycle according to the speed limit; thus, it can be realized that every cycle moves one cell to the downstream cell when there is no congestion. Meanwhile, the length of all the cell is controlled to a similar level and uses an integer number of cells. Finally, based on the results of multiple trial calculations, the simulation takes a time period T of 20 s.

4.2. Road Network Vulnerability Evaluation Results

4.2.1. Vulnerability Evaluation Results under Complete Failure. Figure 5(a) shows the cumulative index changes of the road network vulnerability when the main section of the Bao'an Central Area completely fails, reflecting the overall time loss ratio of all travelers in the region since the event occurred relative to the undisturbed situation.

It can be seen from Figure 5(a) that the cumulative vulnerability curve shows two kinds of trends. One as in situation 1, its cumulative vulnerability value gradually increases to about 0.10 since the event occurs and then tends to be stable. In the others as in situations 2, 3, and 4, the cumulative vulnerability values have increased to a greater extent and produced more obvious signs of recovery. The cumulative vulnerability value of situation 4 is the largest, and its peak value reaches 0.28.

During the period of continuous impact of the event, the vulnerability index value is significantly higher than other situations. The recovery efficiency of situation 2 is relatively high, and the slope of the cumulative vulnerability curve in the recovery phase is significantly higher than in other situations. Corresponding the invalid road link of each situation to the road network, it can be found that when the contact link of Bao'an Avenue and Guangshen Highway fails, more overall time loss is generated and the recovery speed is slow.

Figure 5(b) shows the time-varying index of road network vulnerability when the main link of Bao'an Central Area fails. This index indicates the traveler's time loss in the road network at each time period since the event occurrence. This index eliminates the cumulative effect since the occurrence of the event and directly reflects the consequences of the event at the current time.

A similar conclusion to Figure 5(b) can be obtained from (a). It is worth noting that the initial impact of situation 1 is less than situation 2 at the peak of each curve, but the subsequent sustained impact is basically maintained above situation 2. It is indicated that the main impact periods of different road links are different, and the criticality of the two links needs to be discussed differently based on the continuous impact time of the events.

At the maximum peak of each curve, the initial impact of situation 1 is less than that of situation 2, but the subsequent continuous impact is basically maintained above situation 2. Thus, it may neglect the operational state of the road

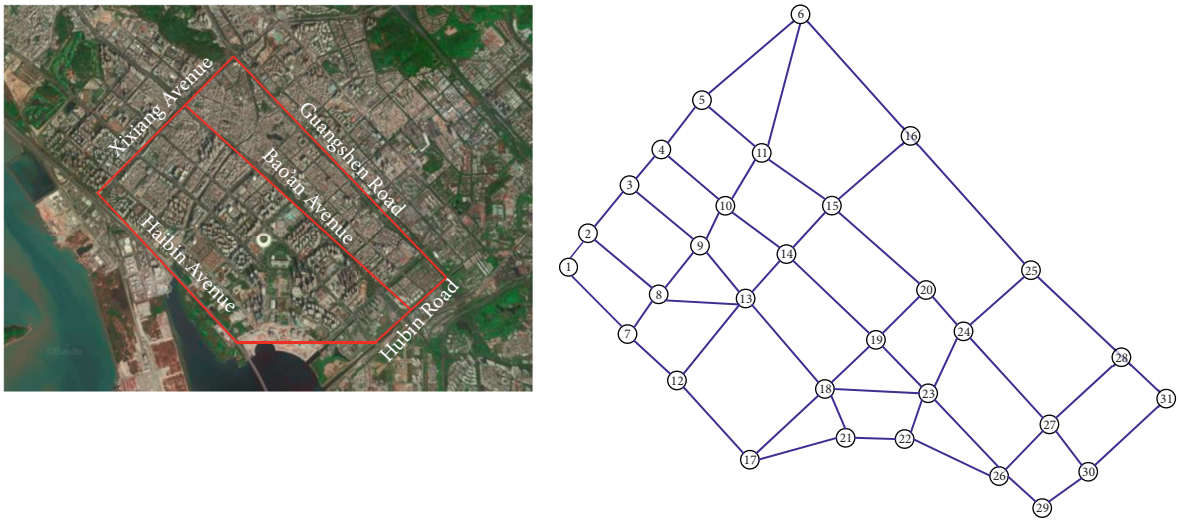

(a) (b)

Figure 4: Example road network structure diagram. The left figure shows the actual layout of the road network in Bao'an Central Area, and the right figure shows that the abstraction is the road network structure.

Table 1: Main interference situation setting table.

Interference situation	Links	Nodes	Number of lanes	Degree of interference
Situation 1	Guangshen Highway (Xixiang Avenue-Chuangye 1st Road)	6⟶25	4 lanes	Complete failure
Situation 2	Bao'an Avenue (Xin'an 6th Road-Yu'an Road)	15⟶20	4 lanes	Complete failure
Situation 3	Bao'an Avenue (Chuangye 1st Road-Xin'an 1st Road)	24⟶27	4 lanes	Complete failure
Situation 4	Chuangye 1st Road (Guangshen Highway-Bao'an Avenue)	24⟶25	3 lanes	Complete failure
Situation 5	Chuangye 1st Road (Guangshen Highway-Bao'an Avenue)	24⟶25	3 lanes	Two-lane failure
Situation 6	Chuangye 1st Road (Guangshen Highway-Bao'an Avenue)	24⟶25	3 lanes	One-lane failure

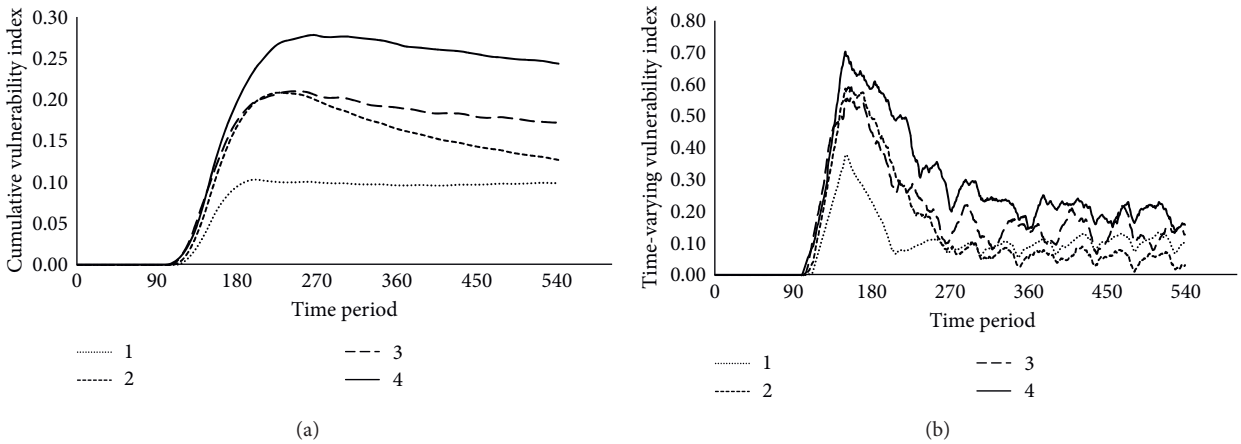

(a) (b)

Figure 5: Vulnerability variation diagram under link complete failure. (a) shows the cumulative vulnerability when the main section of the Bao'an Central Area completely fails, and (b) shows the time-varying vulnerability. (a) Cumulative vulnerability. (b) Time-varying vulnerability.

network in the disordered phase initially affected by the event if applying static indicators only.

The vehicle arrival rate is used to analyze the road network flow variation. It can be visually observed from Figure 6 that the vehicle arrival rate in the disordered phase has dropped significantly in various interference situations, significantly in situations 3 and 4; see Figures 6(a) and 6(b). This corresponds to the obvious rising phase of the time-

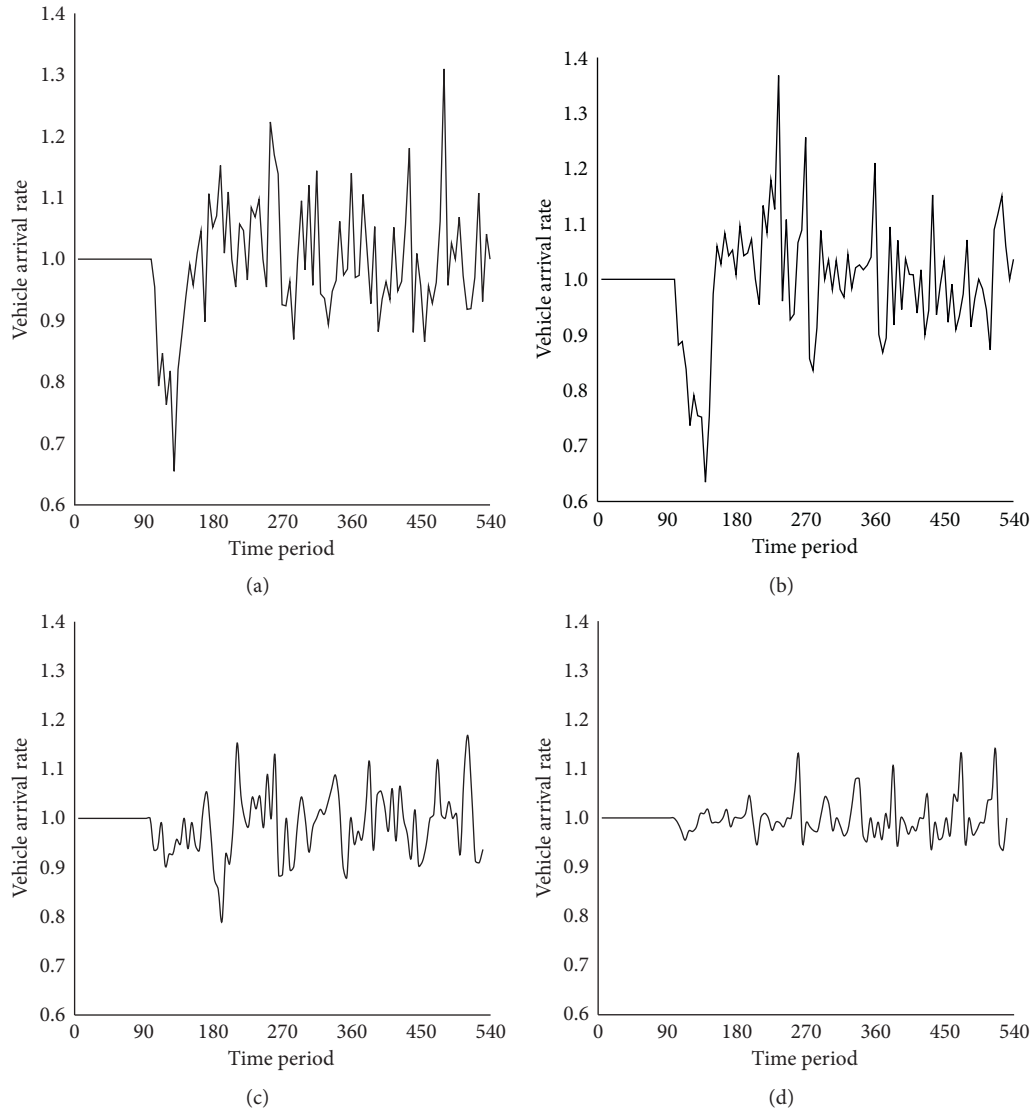

Figure 6: Vehicle arrival rate diagram under complete or partial failure. (a) Situation 3 and (b) situation 4 of complete failure show significant fluctuations. (c) Situation 5 and (d) situation 6 of partial failure situation show flat fluctuations. (a) Situation 3. (b) Situation 4. (c) Situation 5. (d) Situation 6.

varying peak and cumulative vulnerability of each interference situation at the initial stage of the event. The vehicle arrival rate of situations 3 and 4 still maintains a large fluctuation as time passes; that is, the unstable fluctuation of traffic flow makes the time-varying network vulnerability also maintained at a relatively high level.

According to the partial failure situation (see Figures 6(c) and 6(d)), the vehicle arrival rate curves are different from that of complete failure, there is no obvious impact on the disordered phase, and the fluctuation of the period impact amount is small. Situation 6 is even maintained at a level that is comparable to the noninterference situation. The vehicle could still travel to the destination along the original route since the road link is not interrupted in situation 5, so that the vehicle arrival rate does not observe a significant drop in the early stage of the event. After the event occurred for about 100 time periods, the arrival rate shows a large decline. This is because the formation of congestion needs to go through a process after the partial failure of the road. The impact on traffic flow is gradually shown up after the congestion is basically formed.

4.2.2. Vulnerability Evaluation Results of Partial Failure. A further discussion is made based on selecting situation 4 which has a relatively high vulnerability value throughout the simulation. By setting the road partial failure situation from the failed road link 24⟶25 in situation 4 as situations 5 and 6, the road network vulnerability under different interference levels is discussed.

The single-lane failure of the road link can barely expose the vulnerability of the road network (Figure 7). Because the minimum travel time of the link 24⟶25 increases due to the single-lane failure, the link will not become the shortest path

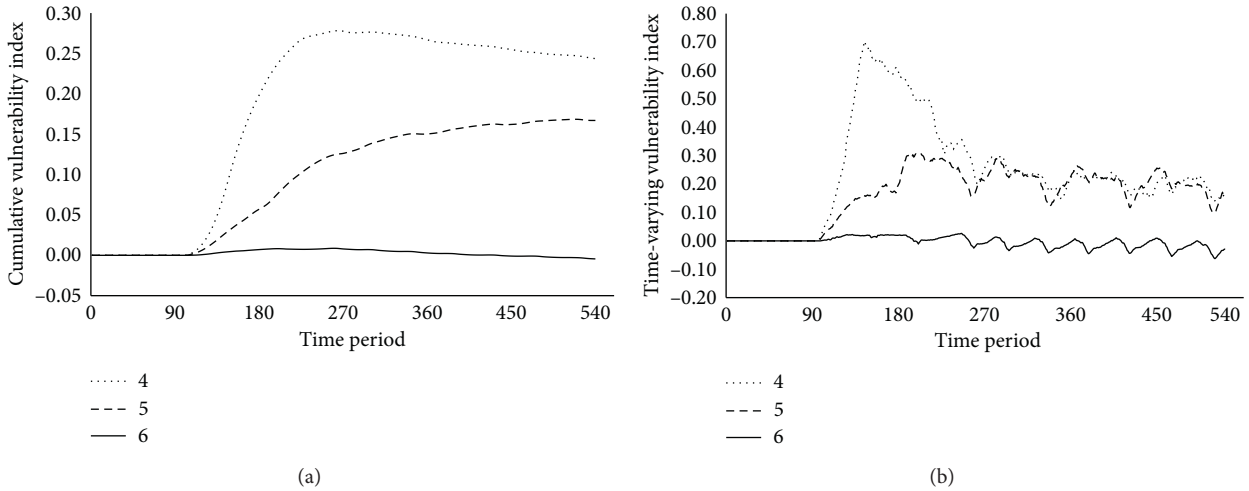

Figure 7: Vulnerability variation diagram under link partial failure. (a) Cumulative vulnerability when setting the road link 24⟶25 failed. (b) Time-varying vulnerability. (a) Cumulative vulnerability. (b) Time-varying vulnerability.

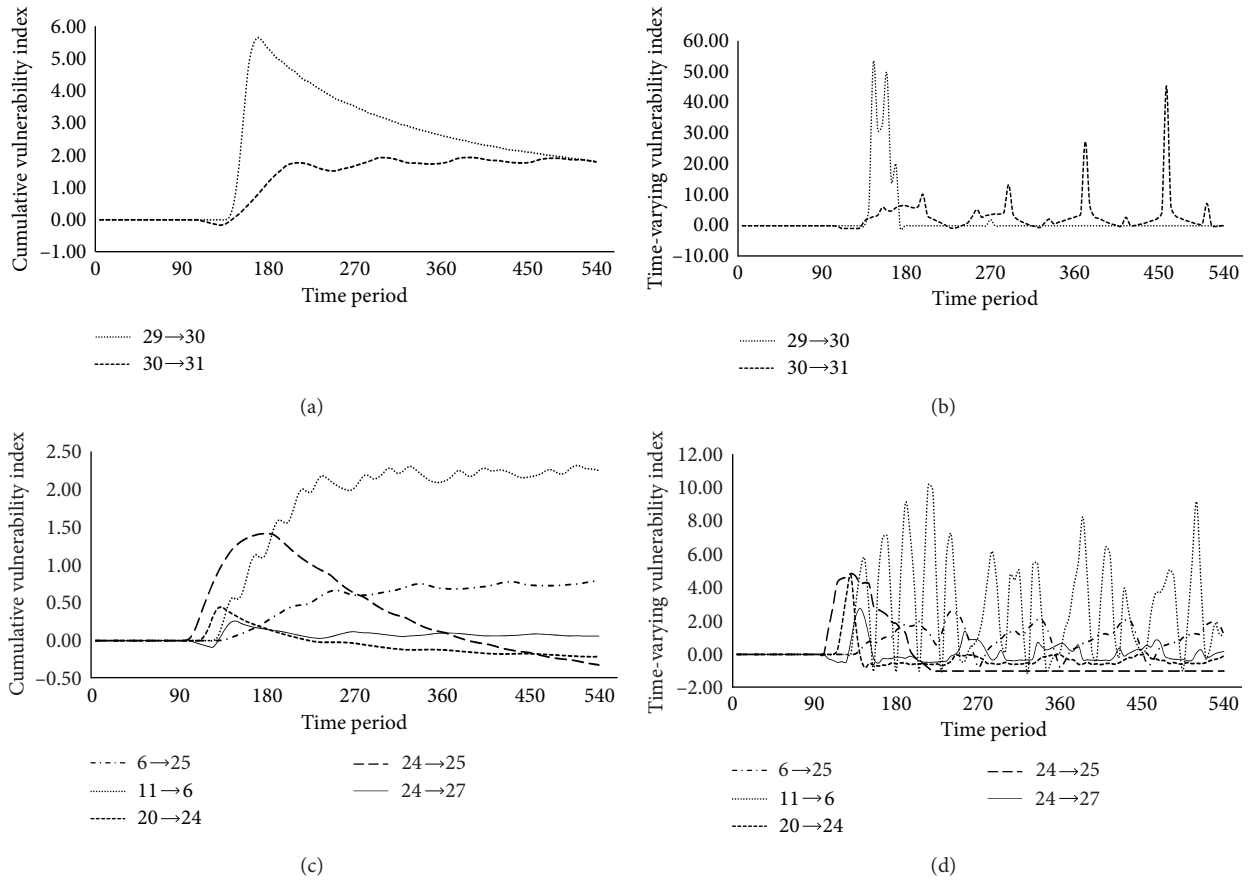

Figure 8: Individual link vulnerability variation. (a, b) Cumulative and time-varying vulnerability under severe impact. (c, d) Cumulative and time-varying vulnerability under general impact. (a) Cumulative vulnerability under severe impact. (b) Time-varying vulnerability under severe impact. (c) Cumulative vulnerability under general impact. (d) Time-varying vulnerability under general impact.

for some travel demand, so that the traffic volume of the link is more stable compared with the noninterference situation, and the road network vulnerability has also decreased.

As Figure 7(b) shows, the initial impact of two-lane failure (scenario 5) is much lower than that of road section complete failure (scenario 4), but the continuous impact

of the two is basically the same. Using static indicators to compare the vulnerability indicators of the two equilibrium states may lead to conclusions that the vulnerabilities of the two situations are similar, which is inaccurate.

4.3. Individual Link Vulnerability Evaluation Results. It is not convenient to list the evaluation results of all the links under all interference situations since there are many links in the example road network. Therefore, take the situation with the highest vulnerability value in the vulnerability evaluation of the former road network as the evaluation object, giving the evaluation result in which the link vulnerability changes significantly under this situation.

Figure 8 shows the vulnerability index variation of the road links with large vulnerability values in situation 4, depending on the degree of each link impact. Obviously, links 29⟶30 and 30⟶31 are severely impacted, and the impact is even higher than the direct event-occurred link 24⟶25. Among them, the influence of the link 29⟶30 is mainly in the disorder stage, and 30⟶31 is affected multiple times during the event impact, which is mainly because the travelers alternately select the shortest path and the second shortest path with the traffic flow evolution, causing link congestion to be formed several times and gradually dissipated.

The time-varying vulnerability of the road link 11⟶6 shows a large fluctuation, and the cumulative vulnerability also has risen with fluctuations. This repeated fluctuation of time-varying vulnerability is also caused by the traveler's alternately selection between the shortest path and the second shortest path.

The two vulnerability index values on the event-occurred link 24⟶25 rise sharply in the disordered phase and decline gradually in the recovery phase. In addition, the time-varying vulnerability of this link is maintained at a lower position after the vehicle is evacuated, and the cumulative vulnerability is also gradually reduced correspondingly. The two vulnerability index values of the links 20⟶24 and 24⟶27 have a small increase with fluctuations in the disordered phase and then quickly return to the low position and enter a new stable state. This change is mainly due to the fact that the two links connect the upstream nodes of the event-occurred link 24⟶25, undertaking the task of evacuating the link traffic flow. Therefore, the vulnerability value in the disordered phase has a large increase obviously and then gradually enters a new equilibrium state after the vehicle evacuation is completed.

5. Conclusions

The vulnerability evaluation of the example road network is carried out, and the dynamic change law of vulnerability is summarized. The model is used to evaluate the vulnerability of road network and link from the two aspects of complete failure and partial failure. The specific research results and conclusions obtained are as follows:

(1) The impact of interference events usually includes a large increase in the time-varying vulnerability value in the disordered phase and then gradually returns to the low level in the recovery phase. The change in cumulative vulnerability value is mainly reflected in the significant increase in the disordered phase and the gradual decline or substantial stability after the evolution into the recovery phase.

(2) Comparing the evaluation results of the road network and individual link, it is found that the road network vulnerability change is relatively flat, and the influence of individual link has the order of influence of event-occurred link, adjacent road links, and similar functional links. Therefore, the road clearing and traffic guidance should be carried out according to the specific conditions of each stage during the dynamic process, strengthening the traffic guidance for the direct event-occurred link and then the similar functional links to avoid repeated congestion.

(3) Comparing the results of complete failure and partial failure of the road, it is found that the interfering event will not have a significant impact on the road network vulnerability when the road has sufficient spare capacity. When the spare capacity of the road link is insufficient, the complete failure of the road causes a greater initial impact. Therefore, it is necessary to maintain a certain traffic capacity for the road links to avoid the vehicles from rushing into adjacent road links in a short period of time.

(4) From the perspective of road traffic flow, when the main road with large traffic flow fails, the road network has a large cumulative vulnerability and a greater time-varying vulnerability during the disordered phase. Therefore, prioritizing the smooth flow of major roads can weaken the impact of road network vulnerability exposure.

(5) From the perspective of network topology, the less the spare capacity or the number of alternative road links, the higher the vulnerability of the road link. Therefore, improving the density of the road network and improving the redundancy of the road network from the topological level can also improve the ability of the road network to resist interference events.

In terms of the universality, it should be noted that lessons from this study could not be generalized to regions like the US or Europe where urban traffic condition is different from that in China. However, for some developing countries, our findings have potential to provide some reference comparably, especially for rapid urbanizing and renewing cities in southeast Asia, with similar traffic condition and road structure to China. The dynamic road vulnerability is complex and the data from Shenzhen city are of limited size, which calls for more context-sensitive and place-based research to supplement the existing knowledge in the future. Our findings could contribute to guiding

sustainable development of integrated transport planning for these developing countries.

For future study, the CTM will be integrated with other transportation networks. Improved versions of this model will consider the elastic demand of traffic travel and the cognitive error of the user since only the complete failure or partial failure of an individual link was considered. The multilink combination failure caused by severe interference events can be studied in the future.

Data Availability

The data used to support the findings of this study are available from the corresponding author upon request.

Conflicts of Interest

The authors declare no conflicts of interest.

Acknowledgments

This research was funded by the National Natural Science Foundation of China, Grants nos. 71974043 and 91846301.

References

[1] K. Berdica, "An introduction to road vulnerability: what has been done, is done and should be done," *Transport Policy*, vol. 9, no. 2, pp. 117–127, 2002.

[2] G. M. D'este and M. A. P. Taylor, "Network vulnerability: an approach to reliability analysis at the level of national strategic transport networks," in *Proceedings of the 1st International Symposium on Transportation Network Reliability (INSTR)*, May 2003.

[3] L.-G. Mattsson and E. Jenelius, "Vulnerability and resilience of transport systems - a discussion of recent research," *Transportation Research Part A: Policy and Practice*, vol. 81, pp. 16–34, 2015.

[4] Y. Gu, X. Fu, Z. Liu et al., "Performance of transportation network under perturbations: reliability, vulnerability, and resilience," *Transportation Research Part E: Logistics and Transportation Review*, vol. 133, 2020.

[5] K. Sugishita and Y. Asakura, "Citation network analysis of vulnerability studies in the fields of transportation and complex networks," *Transportation Research Procedia*, vol. 47, pp. 369–376, 2020.

[6] M. G. H. Bell, "The use of game theory to measure the vulnerability of stochastic networks," *IEEE Transactions on Reliability*, vol. 52, no. 1, pp. 63–68, 2003.

[7] M. G. H. Bell, U. Kanturska, J. D. Schmocker et al., "Attacker-defender models and road network vulnerability," *Philosophical Transactions of The Royal Society A: Mathematical, Physical and Engineering Sciences*, vol. 366, no. 1872, pp. 1893–1906, 2008.

[8] M. G. H. Bell, A. Fonzone, and C. Polyzoni, "Depot location in degradable transport networks," *Transportation Research Part B: Methodological*, vol. 66, pp. 148–161, 2014.

[9] M. G. H. Bell, F. Kurauchi, S. Perera, and W. Wong, "Investigating transport network vulnerability by capacity weighted spectral analysis," *Transportation Research Part B: Methodological*, vol. 99, pp. 251–266, 2017.

[10] J. Pan, M. G. H. Bell, K. F. Cheung et al., "Identifying container shipping network bottlenecks along china's maritime silk road based on a spectral analysis," *Maritime Policy & Management*, vol. 48, no. 2, 2020.

[11] A. Candelieri, B. G. Galuzzi, I. Giordani, and F. Archetti, "Vulnerability of public transportation networks against directed attacks and cascading failures," *Public Transport*, vol. 11, no. 1, pp. 27–49, 2019.

[12] B. Abdulla and B. Birgisson, "Characterization of vulnerability of road networks to random and nonrandom disruptions using network percolation approach," *Journal of Computing in Civil Engineering*, vol. 35, no. 1, 2020.

[13] M. Chen and H. Lu, "Analysis of transportation network vulnerability and resilience within an urban agglomeration: case study of the greater Bay area, China," *Sustainability*, vol. 12, no. 18, p. 7410, 2020.

[14] M. A. P. Taylor, S. V. C. Sekhar, and G. M. D'Este, "Application of accessibility based methods for vulnerability analysis of strategic road networks," *Networks and Spatial Economics*, vol. 6, no. 3-4, pp. 267–291, 2006.

[15] A. Chen, C. Yang, S. Kongsomsaksakul, and M. Lee, "Network-based accessibility measures for vulnerability analysis of degradable transportation networks," *Networks and Spatial Economics*, vol. 7, no. 3, pp. 241–256, 2007.

[16] E. Jenelius, T. Petersen, and L.-G. Mattsson, "Importance and exposure in road network vulnerability analysis," *Transportation Research Part A: Policy and Practice*, vol. 40, no. 7, pp. 537–560, 2006.

[17] E. Jenelius, L.-G. Mattsson, and D. Levinson, "Traveler delay costs and value of time with trip chains, flexible activity scheduling and information," *Transportation Research Part B: Methodological*, vol. 45, no. 5, pp. 789–807, 2011.

[18] E. Jenelius, "Network structure and travel patterns: explaining the geographical disparities of road network vulnerability," *Journal of Transport Geography*, vol. 17, no. 3, pp. 234–244, 2009.

[19] E. Jenelius and L.-G. Mattsson, "Road network vulnerability analysis of area-covering disruptions: a grid-based approach with case study," *Transportation Research Part A: Policy and Practice*, vol. 46, no. 5, pp. 746–760, 2012.

[20] M. A. P. Taylor and fnm Susilawati, "Remoteness and accessibility in the vulnerability analysis of regional road networks," *Transportation Research Part A: Policy and Practice*, vol. 46, no. 5, pp. 761–771, 2012.

[21] E. Jenelius and L.-G. Mattsson, "Road network vulnerability analysis: conceptualization, implementation and application," *Computers, Environment and Urban Systems*, vol. 49, pp. 136–147, 2015.

[22] J. Ding, S. Gao, E. Jenelius et al., "Routing policy choice set generation in stochastic time-dependent networks, transportation research record," *Journal of the Transportation Research Board*, vol. 2466, no. 1, pp. 76–86, 2014.

[23] M. Bababeik, M. M. Nasiri, N. Khademi, and A. Chen, "Vulnerability evaluation of freight railway networks using a heuristic routing and scheduling optimization model," *Transportation*, vol. 46, no. 4, pp. 1143–1170, 2019.

[24] G. Gecchele, R. Ceccato, and M. Gastaldi, "Road network vulnerability analysis: case study considering travel demand and accessibility changes," *Journal of Transportation Engineering*, vol. 145, no. 7, pp. 05019004.1–05019004.10, 2019.

[25] D. M. Scott, D. C. Novak, and F. Guo, "Network robustness index: a new method for identifying critical links and evaluating the performance of transportation networks," *Journal of Transport Geography*, vol. 14, no. 3, pp. 215–227, 2006.

[26] C. Balijepalli and O. Oppong, "Measuring vulnerability of road network considering the extent of serviceability of critical road links in urban areas," *Journal of Transport Geography*, vol. 39, pp. 145–155, 2014.
[27] E. Alex, B. James, A. Kay et al., "Vulnerability assessment methodology for Swiss road network," *Transportation Research Record*, vol. 2137, no. 1, pp. 118–126, 2009.
[28] B. Y. Chen, W. H. K. Lam, A. Sumalee, Q. Li, and Z.-C. Li, "Vulnerability analysis for large-scale and congested road networks with demand uncertainty," *Transportation Research Part A: Policy and Practice*, vol. 46, no. 3, pp. 501–516, 2012.
[29] X. Xiangdong, C. Anthony, J. Sarawut et al., "Transportation network redundancy: complementary measures and computational methods," *Transportation Research Part B Methodological*, vol. 114, pp. 68–85, 2018.
[30] O. Cats and E. Jenelius, "Dynamic vulnerability analysis of public transport networks: mitigation effects of real-time information," *Networks and Spatial Economics*, vol. 14, no. 3-4, pp. 435–463, 2014.
[31] E. Jenelius, "Incorporating dynamics and information in a consequence model for road network vulnerability analysis," in *Proceedings of the 3rd International Symposium on Transport Network Reliability (INSTR)*, The Hague, The Netherlands, July 2007.
[32] V. L. Knoop, M. Snelder, and S. P. Hoogendoorn, "Link-level vulnerability indicators for real-world networks," *Transportation Research Part A: Policy and Practice*, vol. 46, no. 5, pp. 843–854, 2012.
[33] S. Kim and H. Yeo, "Evaluating link criticality of road network based on the concept of macroscopic fundamental diagram," *Transportmetrica A: Transport Science*, vol. 13, no. 2, pp. 162–193, 2017.
[34] E. Jenelius and L. G. Mattsson, "Developing a methodology for road network vulnerability analysis," *Nectar Cluster*, vol. 1, pp. 1–9, 2006.
[35] C. F. Daganzo, "The cell transmission model: a dynamic representation of highway traffic consistent with the hydrodynamic theory," *Transportation Research Part B: Methodological*, vol. 28, no. 4, pp. 269–287, 1994.
[36] C. F. Daganzo, "The cell transmission model, part II: network traffic," *Transportation Research Part B: Methodological*, vol. 29, no. 2, pp. 79–93, 1995.
[37] H. Szeto and Y. S. Wai, "A cell-based variational inequality formulation of the dynamic user optimal assignment problem," *Transportation Research Part B: Methodological*, vol. 36, no. 5, pp. 421–443, 2002.
[38] W. Y. Szeto and H. K. Lo, "A cell-based simultaneous route and departure time choice model with elastic demand," *Transportation Research Part B: Methodological*, vol. 38, no. 7, pp. 593–612, 2004.
[39] Y. Jiang, Y. Wang, W. Y. Szeto et al., "Probabilistic assessment of network vulnerability with equilibrium flows by metaheuristics," *International Journal of Sustainable Transportation*, vol. 3, 2020.